QUANTIFYING GPS BASE STATION INTERFERENCE FROM LOWER TROPOSPHERIC WILDFIRE CONDITIONS: GNSS AS REMOTE SENSING

by

JERAD KING

ENVIRONMENTAL GEOSCIENCE

BAILEY JONES

GIST

JACKSON STILLWATER

ENVIRONMENTAL GEOSCIENCE

BEN SCHRADER

ENVIRONMENTAL STUDIES

GEOG/GEOL 352
Global Navigation Satellite System for Geosciences
Texas A&M University

ABSTRACT

Amid a changing climate and growing risk of natural hazards, GNSS can be an important tool for understanding climate mitigation and adaptation. Remote sensing using GPS offers a potential for studying wildfires with the benefit of a high temporal resolution and a continuous dataset. Utilizing Receiver Independent Exchange (RINEX) data from Pacific Boundary Observatory (PBO) base stations in California, the signal to noise ratio (SNR) can be used to assess the localized tropospheric interference caused by wildfire conditions. The benefit of using RINEX data relates to the ability to gather SNR data from a continuously operating reference station (CORS) with specific parameters. Relevant parameters include the azimuth of GPS signal reception as well as the angle of incidence of the intercepted signal.

Following the site selection, the 2020 August Complex Fire, and acquisition of RINEX data, the SNR component is processed with the appropriate azimuth and signal angle parameters. The extracted SNR data is then processed to carry out statistical analysis and produce interpretable graphic products. SNR data was normalized and tested against data from the same base station during non-wildfire conditions. To properly isolate lower tropospheric GPS interference from wildfire conditions, the control data was selected from the same dates of the prior year. This controls for any major seasonal variability of meteorological conditions. Additionally, the dataset is continuous and statistically normalized, relieving the potential for random ionospheric interference as a confounding variable. The goal of this study is to quantify and assess the significance of wildfire interference in L1 band lower tropospheric propagation and evaluate the feasibility of this methodology to remotely sense wildfires.

1. INTRODUCTION

The applications of using SNR data from GPS base stations as a tool for remote sensing are novel, and their viability for gathering information for different applications is the subject of a growing number of studies. While space and airborne systems are the dominant platforms for acquiring data over a large study area, the proliferation of GNSS and GPS base stations are another potential platform for remote sensing. The focus of this study was to evaluate the efficacy of utilizing signal interference from wildfire induced tropospheric conditions as a method to quantify wildfire intensity. Increasing frequency and intensity of wildfires caused by a changing climate are a persistent threat to vulnerable areas, particularly California, the area of interest for this study (Leman, 2020). Principally, this study will serve as a proof for this method, determining if statistically significant L1 wave attenuation and signal noise can be caused by wildfire tropospheric conditions.

The fundamental property of remote sensing is the study of electromagnetic radiation (EMR) wave propagation. GPS base stations intercept several wavelengths from satellites to receive positioning data that then may be stored and broadcast to a rover. The L1 band broadcasts at 1575.42 MHz with a wavelength of 19.05 centimeters. Compared to the L2 band, operating at 1227.60 Mhz with a wavelength of 24.45 centimeters, the L1 band has a higher vulnerability for interference from atmospheric conditions. The longer wavelength of L2 propagates easier through atmospheric particles. Put simply, longer wavelengths travel through greater densities of mass than shorter wavelengths. CORS base stations store and upload raw signal data contained within RINEX files to public

access websites. Measuring signal interference from the L1 GPS band mimics other applications of EMR remote sensing.

GPS signal to noise ratios have previously not been used to measure the intensity of wildfire induced tropospheric interference, however, similar studies have been conducted to measure other atmospheric conditions. A 2021 study by Yang et al. explored the application of GNSS as remote sensing to measure precipitable water vapor (PWV) in the atmosphere. The delay from GNSS precise point positioning signals operating at millimeter accuracy were analyzed to determine density of PWV in the troposphere (Yang, 2021). Given the similarity in densities between wildfire smoke particulate and PWV, this study serves as a proof for the viability of methodology. A 2008 thesis by Mphale investigated radio wave propagation through bushfire tropospheric conditions. While the length of EMR bands studied by Mphale differ from the L1 band, Mphale hypothesized that ionization of atmospheric particles from the thermal bubble and plume produced by the bushfire lead to measurable attenuation of radio wave signals (Mphale, 2008). Within the context of GNSS as remote sensing, the ionization caused by wildfires could cause interference that is similar to ionospheric interference. A 2017 study by Lau investigated the effect atmospheric particulate matter (PM) from pollution have on the strength of GNSS signals. Lau found that there were only minor impacts from anthropogenic atmospheric pollution of PM 2.5 and PM 10.0, mostly below 1 dB/Hz (Lau, 2017). The maximum density of particulate matter tested in the study was 40 ug/m^3. This differs from wildfire atmospheric conditions, however, as particulate matter densities can exceed 200 ug/m^3 (Li, 2020). Given the greater density of particulate matter

in wildfire smoke, as well as the ionization of particles in the troposphere, L1 wave attenuation is expected to be higher than what was measured by Lau.

The first component of the methodology of this study was site selection. The 2020 August Complex Fire in California was chosen due to its record-breaking size and intensity (Cal Fire, 2021). Additionally, choosing a wildfire in California was advantageous due to the amount of GPS base stations that compose the Plate Boundary Observatory (PBO). Following the selection of GPS base stations in proximity to the extent of the fire, the RINEX data for the days of highest intensity and fire extent were downloaded. Figure 1 shows the geospatial datasets that were used to select appropriate CORS base stations. RINEX data on its own is not directly interpretable and the desired information needs to be processed. The SNR data, often measured in decibels or volts, was extracted from the RINEX file utilizing RTKLIB. RTKLIB generates a file containing time, satellite, elevation angle, azimuth, SNR, and L1 information. Within MATLAB, the parameters for azimuth, elevation angle, and time were specified. The azimuth of signal was chosen based upon the base station's spatial relation to the wildfire. An elevation angle was chosen between 5 and 50 degrees in order to observe trends at higher elevation angles. At a shallow elevation angle, GPS signals must travel through a denser part of the atmosphere, so it is most preferable to detect wildfire interference.

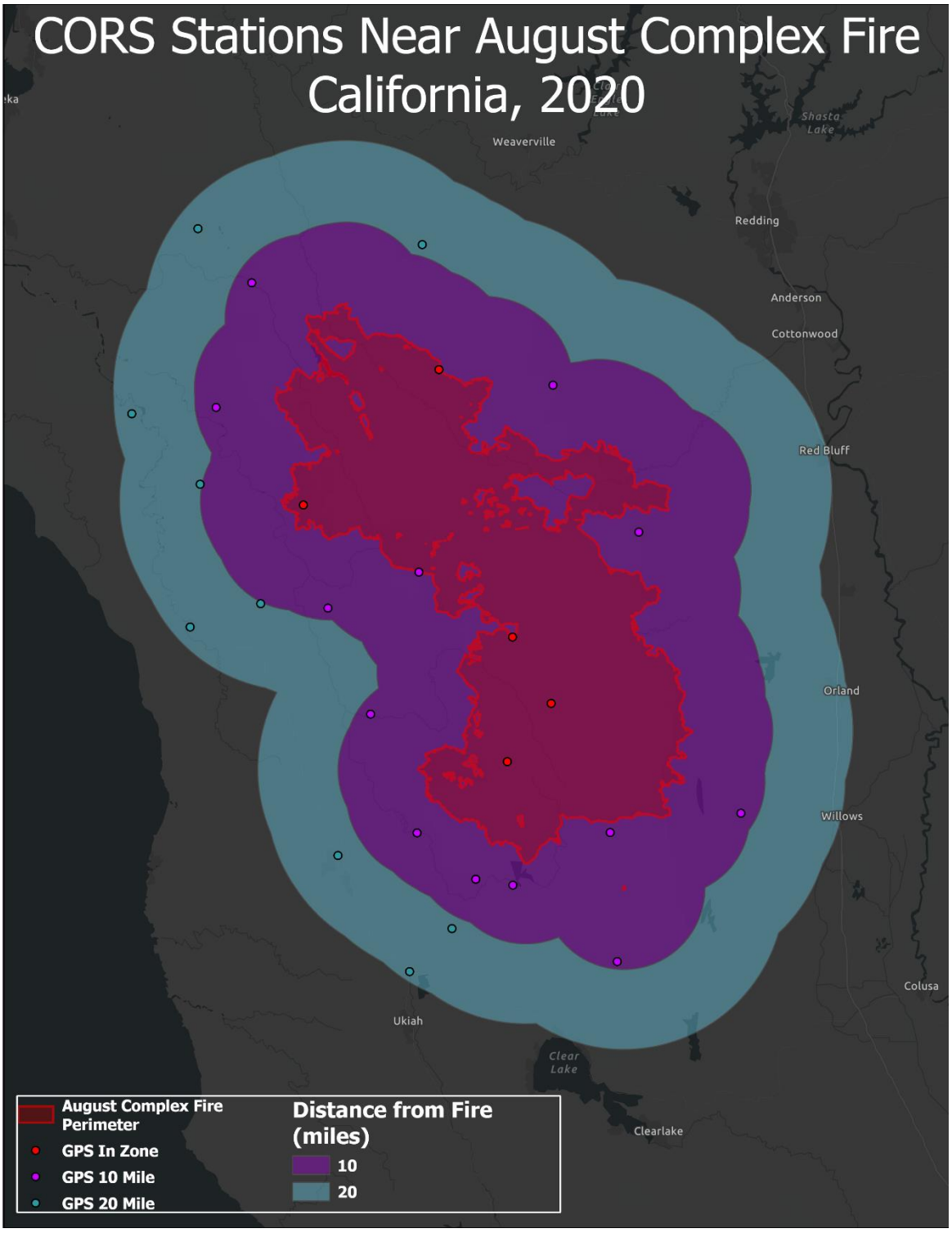

Figure 1: CORS Station Selection and August Complex Fire Extent

Once the SNR data was collected, it was output from RTKLIB into an xls table. The output table was then input into MATLAB for post processing. Statistical tests such as two-tail t tests, RMS, and residuals determined the significant difference between the test group (SNR data from wildfire conditions), and the control group (SNR data from the same base station during non-wildfire conditions). Following the statistical tests, interpretable data products such as graphs and tables were generated in MATLAB to show results.

Results will show a statistically significant difference between non-wildfire and wildfire conditions. The continuous dataset produced from the control group and the experimental group are normalized to account for random variability in signal strength caused by ionospheric interference. Controlling for random variability between the test and control dataset isolated tropospheric interference from random ionospheric interference. The following processed datasets are expected to show a moderate, yet significant, differential between the test and control group. With a p-value of 0.05, the statistical test is expected to reject the null-hypothesis (H_0), indicating a statistically significant difference between SNR of the test group and control group. Figure 2 is an example of a graph produced that compares signal to noise ratios under different conditions. Relevant parameters in the data products indicate that signal angle and azimuth increase the amount of noise in the processed signals. This is the result of EMR wave propagation through a denser part of the atmosphere, with the wildfire dataset indicating a higher noise ratio because of the attenuation caused by the signal traveling through wildfire plumage.

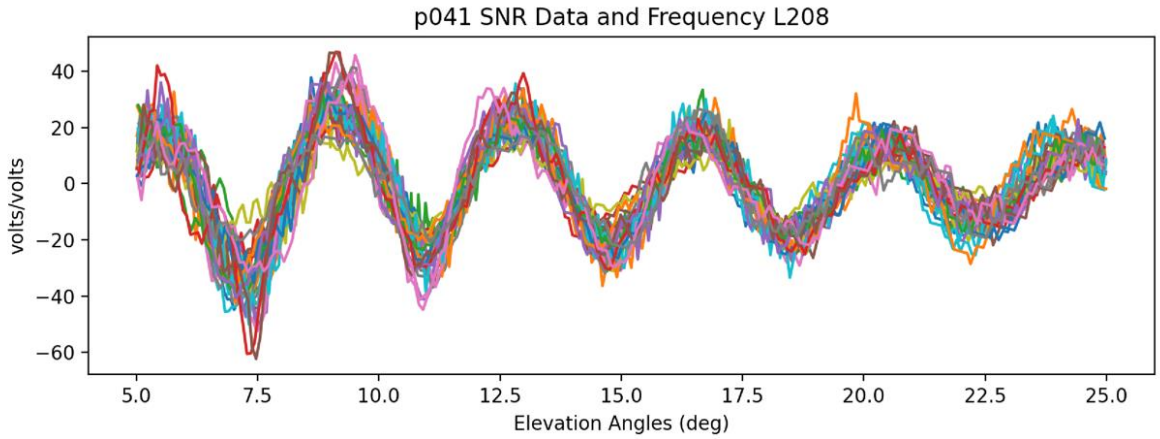

Figure 2: Example of SNR (volts) graphed against elevation angle: Larson, 2021

Future studies can utilize this method to compare the intensity of wildfires with GNSS. After establishing the viability of this method to determine the magnitude of interference produced by tropospheric wildfire conditions there is potential for a new standardized index of wildfire severity based on GNSS. It is important to note that accuracy of GPS receivers is likely not affected by wildfire conditions due to post processing corrections and triangulation of multiple satellites. The parameters for this test were designed to emulate a worst-case scenario for L1 wave propagation without any corrections for error applied. With adequate magnitude of signal noise from wildfire conditions, there is a potential for the construction of an algorithm that measures atmospheric interference in real-time.

2. METHODS

CORS base stations were selected based upon the proximity to the August Complex Fire perimeter. An additional spatial parameter was considered, the distance to fire plumage on August 20th, 2020, day of year (DOY) 230. August 20th was selected due to high relative density of smoke in the region (*NA*,2020). Limitations included data availability for potential base stations on the selected date. Of the eligible base stations, P336 and P190 were selected as the sites have reduced potential multipath error caused by poor line of sight (LOS) from terrain masking. RINEX data was then obtained from NOAA UFCORS for DOY 230 for 2020, wildfire conditions, and DOY 230 for 2019, non-wildfire conditions. Using the same base station as the control SNR group was crucial to control for multipath error as terrain reflection is a dominant source of signal interference below a 25º elevation angle. Figure 1 shows the CORS base station location relative to the fire perimeter, and specified azimuth field of view. The RINEX format contains a continuous dataset for a multitude of GPS observations for a given base station. Of interest was azimuth, elevation angle, and SNR. The RINEX data was then formatted into a readable text document with appropriate parameters using the open-source RTKLIB tool RTKPLOT and read into MATLAB for post-processing and statistical analysis. The statistical tests used include 2-tail T tests, RMS, and calculation of residuals.

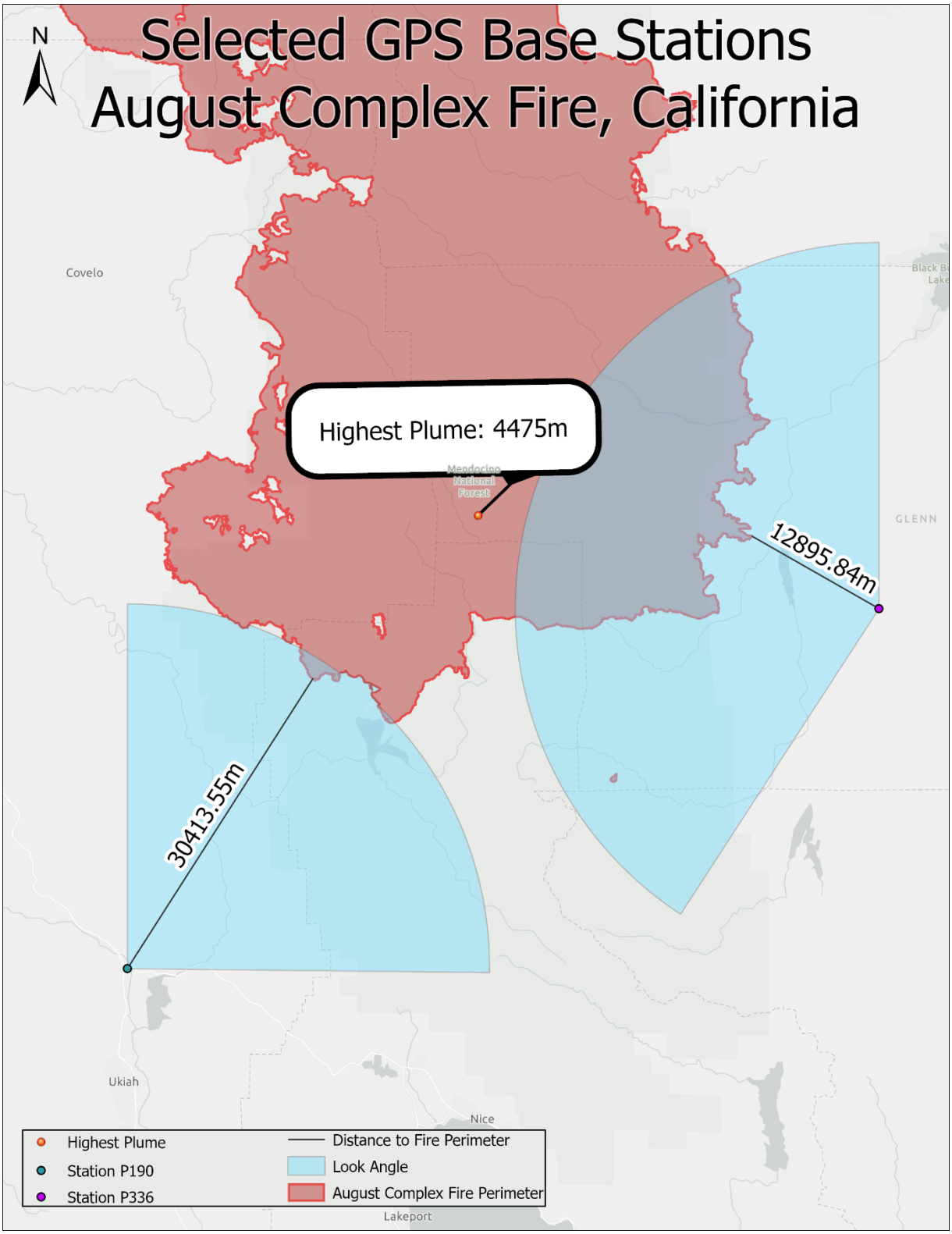

Figure 3: CORS P190 and P336

Following the acquisition of data in RINEX 2.11 format, the data was pre-processed to extract SNR for each base station and date. The open-source GNSS post-processing software package RTKLIB (Takasu,2018) was used to convert the RINEX files into txt files using the "RTKPLOT" tool. The file contained time (GMT), satellite number, azimuth (degrees), elevation (degrees), and SNR (dB/Hz).

The text files were then read into MATLAB 2021b and further processed. To create one to one dimension for control and experimental datasets, the arrays were reshaped to the size of the dataset that was the limiting dimension. In the case of P336, a large portion of data was absent between 0200 and 0500 GMT. Figure 2 displays the missing data in RTKPLOT. To ensure the preservation of important parameters, the experimental and control datasets were sorted by time, and the dimension was reduced to the size of the limiting dataset. This was accomplished using exclusive Boolean logic to index the shared time value, accurate to 30 seconds. A field of view for the base station based on azimuth further reduced the dimensions of the datasets to match desired parameters. This was determined by the azimuth relative to the base station's location in reference to the fire perimeter. The look angle for P190 was 0ºN to 90ºW and for P336 was 200ºS-SW as seen in Figure 1. The resulting array size for P336 was 7,673 x 5 and 4,894 x 5 for P190. This completed the data pre-processing procedure.

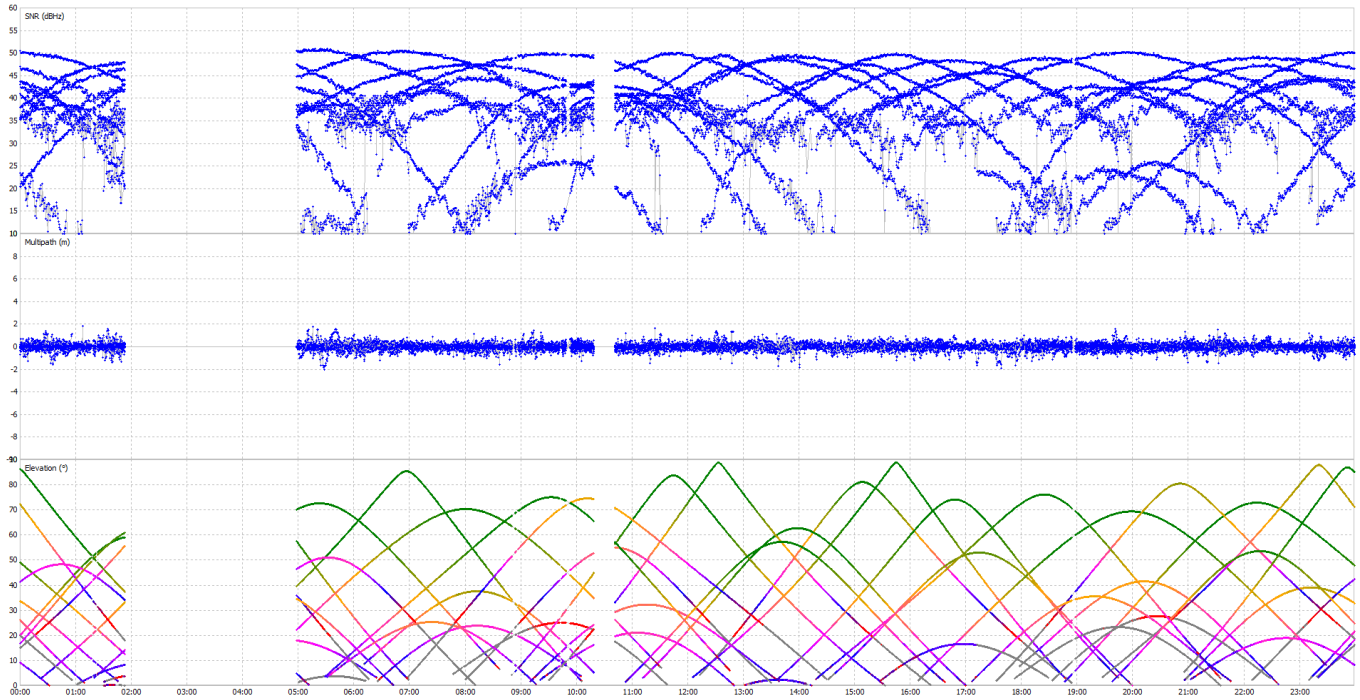

Figure 4a.) 2020 P336 data with 0200 and 0500 GMT with incomplete data in RTKPLOT

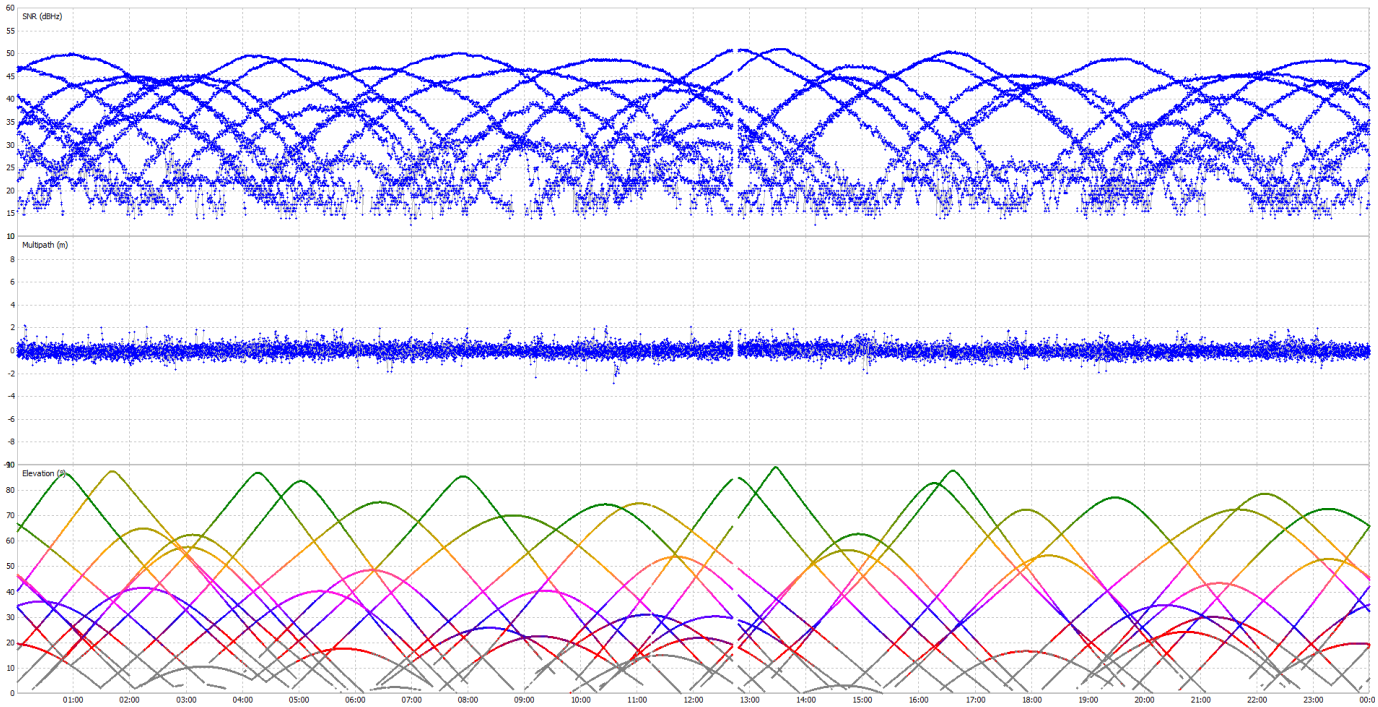

Figure 2b.) 2019 P336 data with minimally absent data in RTKPLOT

Graphing and indexing raw SNR data pre-application of statistical tests was important to establish the presence of initial trends in the dataset. Figure 3 displays the SNR data for 2019 and 2020 as a function of elevation. Figure 4 represents the distributions of SNR according to their frequency in each dataset. The resulting graph displays an expected trend of SNR as signal strength increases with rising elevation angle as atmospheric and multipath error is reduced. A two-tail T test was run on the control vs experimental groups with a rejection of null-hypothesis at a p-value approaching 0. Both datasets produced a strong indication of statistically significant difference between wildfire and non-wildfire conditions.

Table 1.1 and 1.2

P190 SNR (dB/Hz) Summary Statistics

DOY and Year	Mean	Standard Deviation
230, 2019	42.23	4.15
230, 2020	41.61	4.25

P336 SNR (dB/Hz) Summary Statistics

DOY and Year	Mean	Standard Deviation
230, 2019	42.95	3.97
230, 2020	41.68	4.02

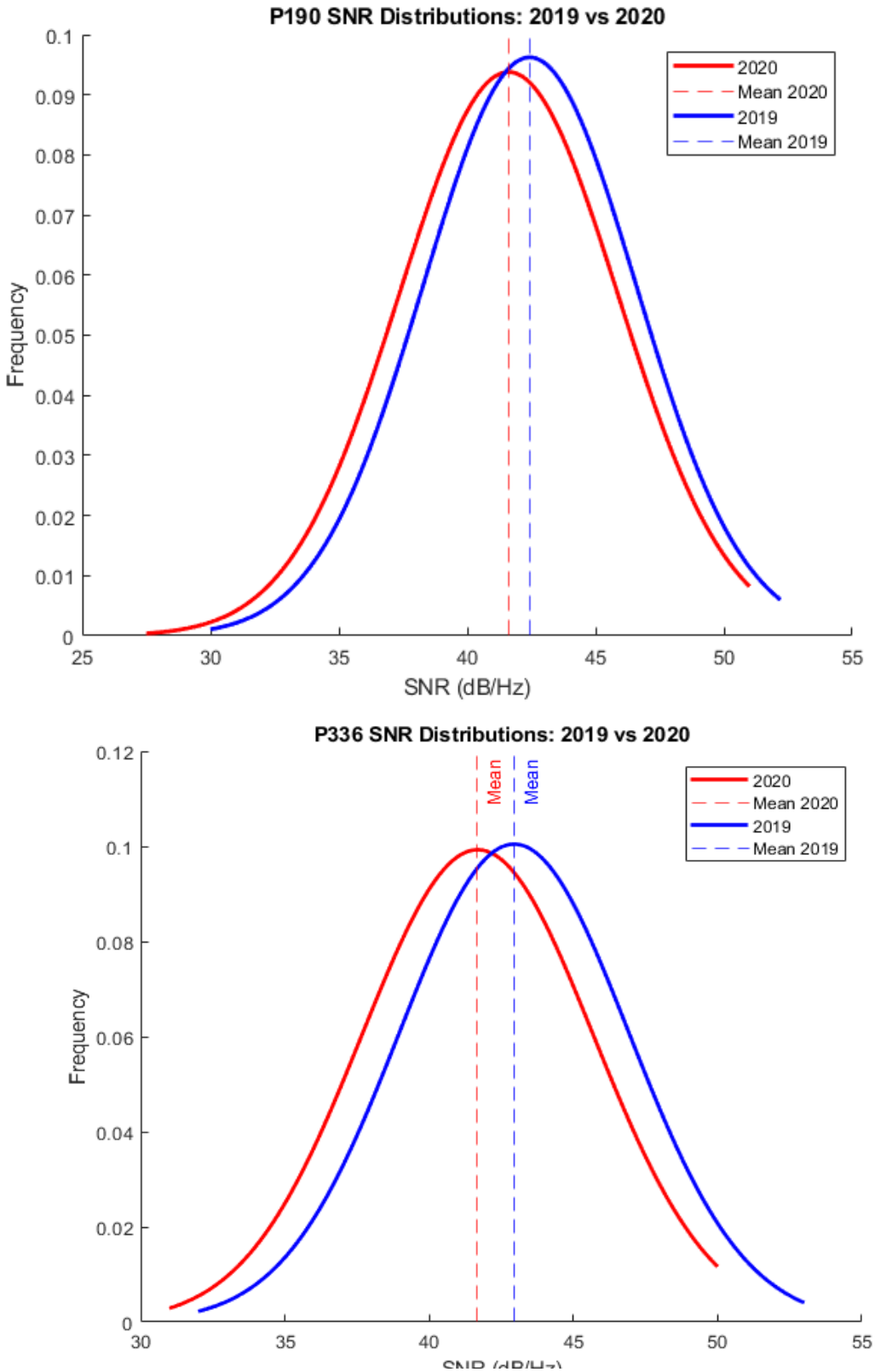

Figure 5 a/b.) Distributions of SNR for P190 and P336

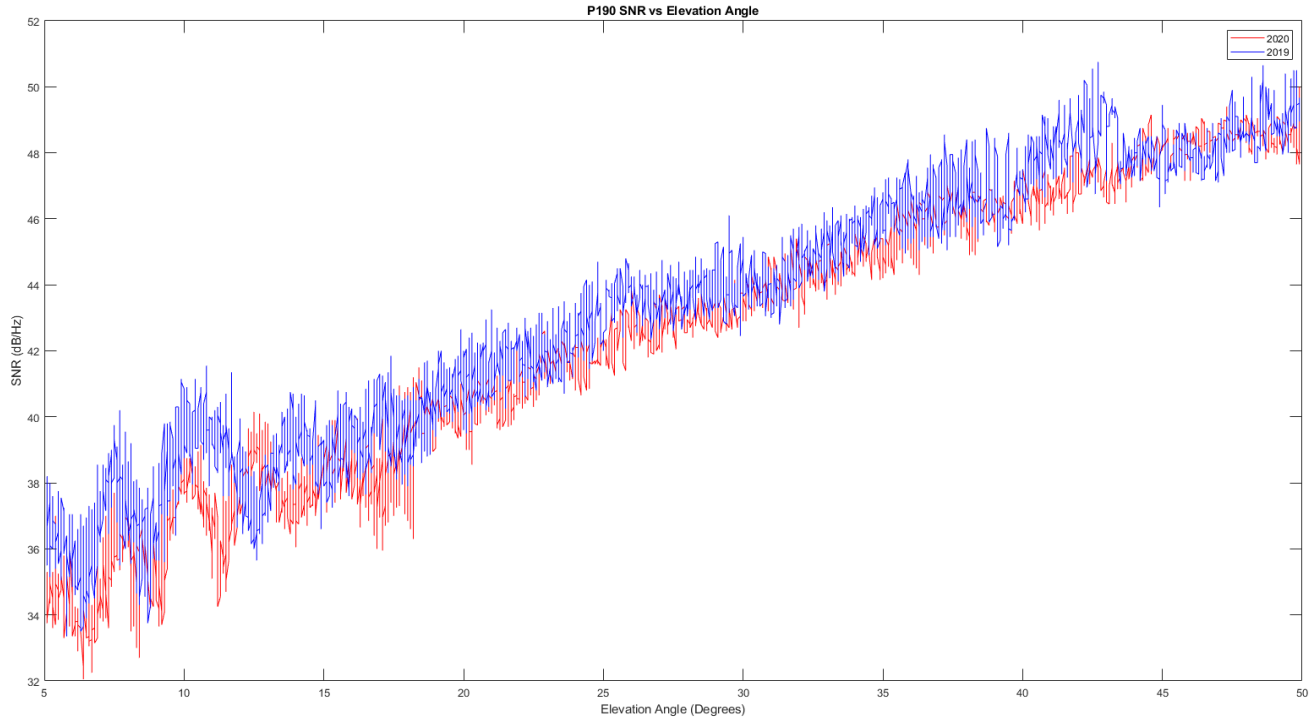

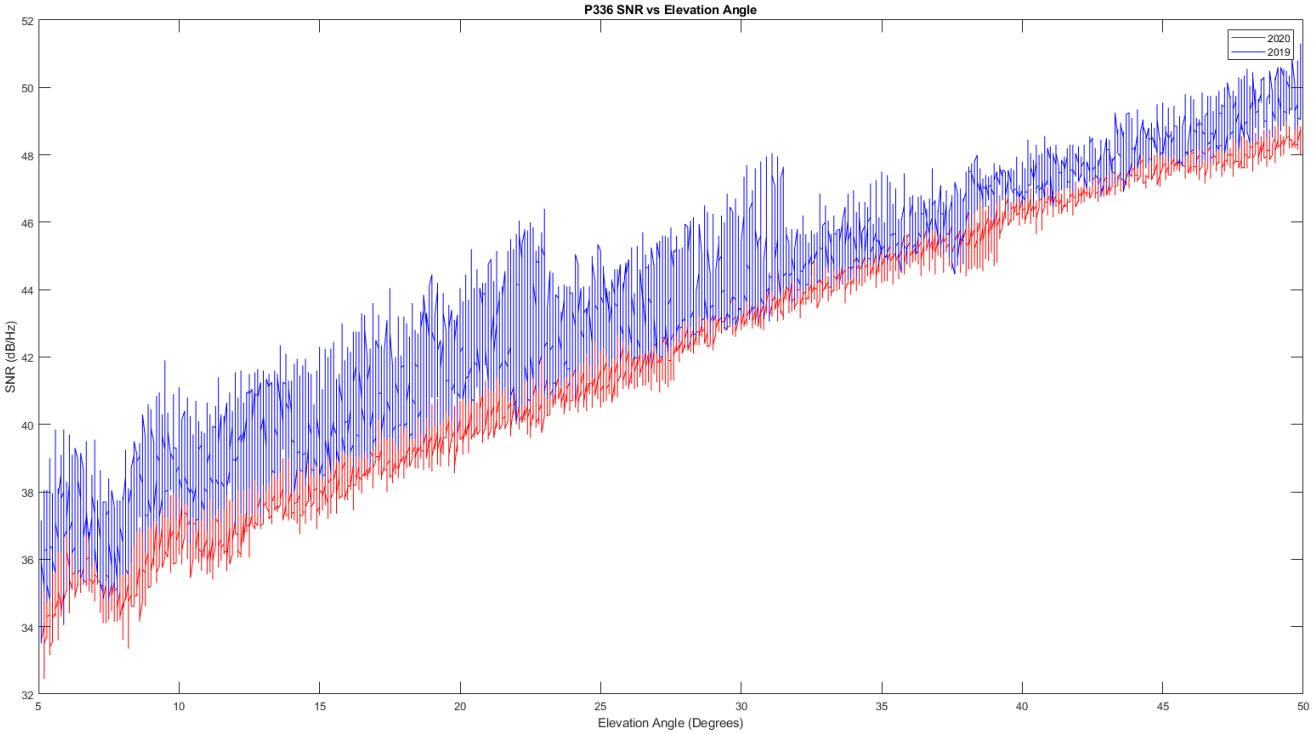

Figure 4 a/b.) SNR graphed against Elevation angle

To normalize the SNR dataset, the RMS (root-mean-square) function was applied to the SNR columns *(*Equation 1*)*. Following this, the residual was calculated for the SNR datasets. This method is similar to Larson's 2017 study which used SNR RMS residuals to detect volcanic eruptions. Significant drops in SNR RMS residuals indicated the occurrence of an event that was measured by L1 signal interference (Larson, 2017). While Larson's study utilized SNR to detect the presence of a volcanic event, the effects of tropospheric conditions from wildfires produce a continuously lower SNR due to constant signal interference. Therefore, the equation was modified so that test condition RMS would represent x_0 in the residual equation $r = x - x_0$, as demonstrated in Equation 2. SNR RMS residuals now indicate distance from control SNR levels. With the modified residual equation now applied, the magnitude of difference in interference may be interpreted. Binomial distributions were produced for RMS residuals. Furthermore, mean and up to 3 standard deviations of the residuals were calculated and indexed. Figure 5 displays the binomial distributions for the SNR RMS residuals.

$$RMS = \sqrt{\frac{1}{n}\sum_{i} x_i^2} \qquad \textit{Equation 1}$$

$$RMS_{residual} = RMS_{test} - RMS_{control} \qquad \textit{Equation 2}$$

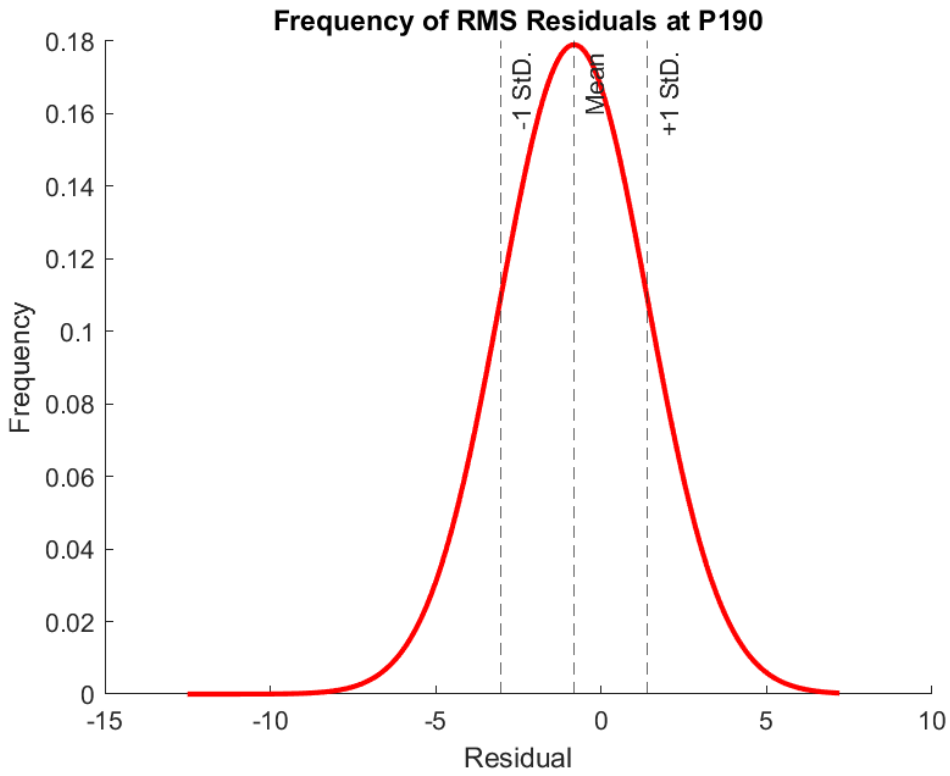

Figure 5a.) SNR RMS residuals at P190

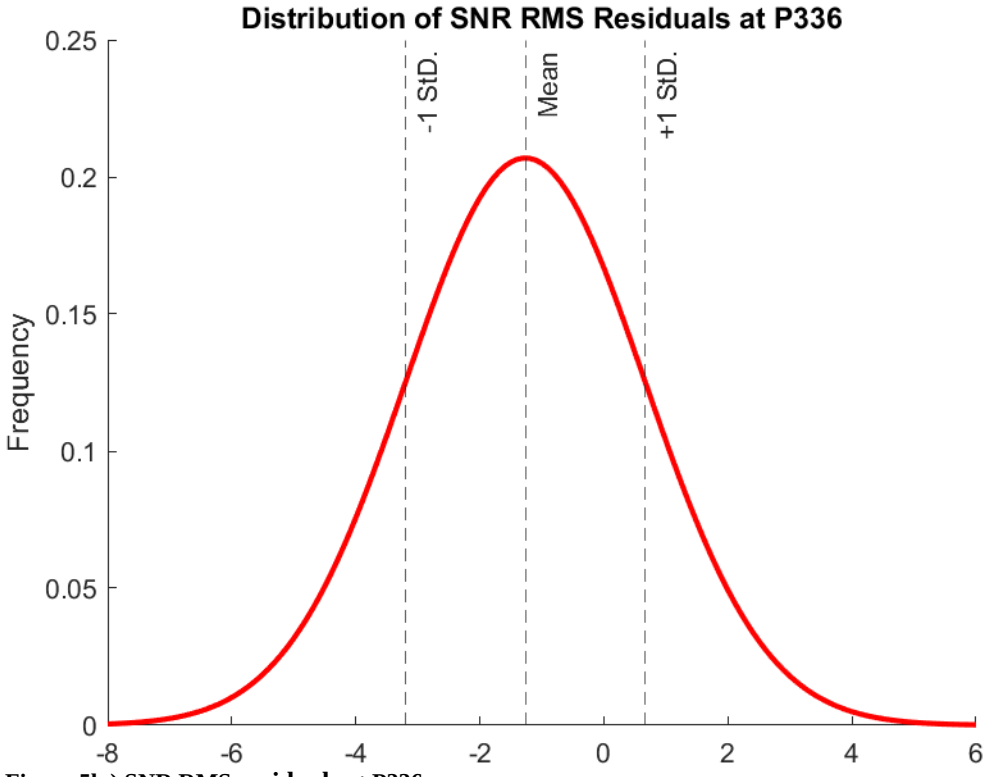

Figure 5b.) SNR RMS residuals at P336

Table 2.1

SNR RMS Residuals Summary Statistics		
Station	Mean	Standard Deviation
P190	-0.82	2.23
P336	-1.27	1.93

With a statistically significant decrease in signal strength established among the elevation variable of the dataset, a semi-empirical model was derived to derive a relationship between base station location, signal interference, and elevation angle. The equation is comprised of the mean elevation angle of RMS residuals that are 3 standard deviations below the mean, and distance to fire plume extent. The result is the approximate altitude of maximum signal interference at the signal to plume intercept. Equation 3 represents the model used. Calculated elevation angle for P336 was 12.34º at a constant distance of 12.9km, and altitude of 2820 meters. P190 produced an elevation angle of 9.15º at a constant distance of 30.4km with an altitude of 4750km. Figure 6 visualizes a 2-dimensional view of the semi-empirical model. Deriving an equation from the data was important to establish a relationship between the location and dominant angles of interference. This model represents an estimation of the altitude at peak L1 signal interference in tropospheric wildfire conditions.

$$i_x = \bar{x} - \left(\sqrt{\frac{\sum(x_i - u)^2}{N}}\right) \times 3 \qquad \theta = \bar{\theta}_{ix} \qquad H = tan(\theta) \times d$$

Equation 3.) Above is the system of equations with i_x indicating SNR residual 3 standard deviations below the mean, θ as elevation angle, d as distance to fire perimeter, and H as height of peak SNR interference at plume intercept.

Table 3.1

Equation 3 Variables and Results for Each Station

Station	$i\square x\square$	θ	d	H
P190	-7.51	9.15º	30.4km	4,750m
P336	-7.05	12.34º	12.9km	2,820m

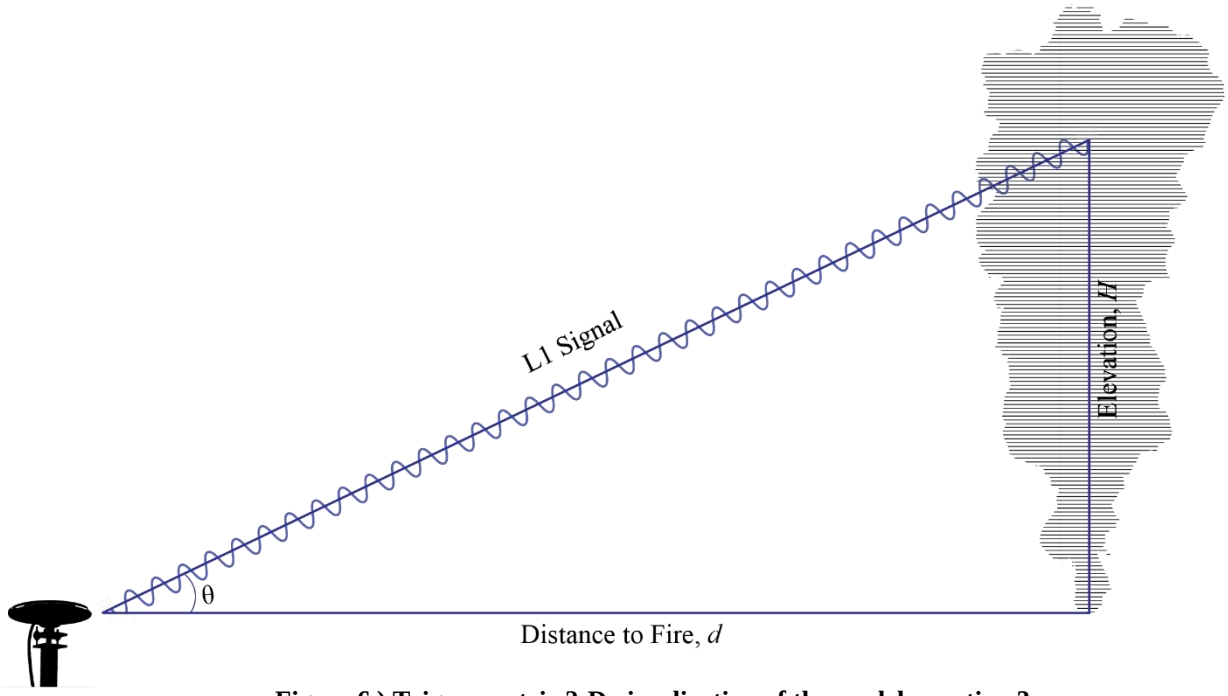

Figure 6.) Trigonometric 2-D visualization of the model equation 3

3. RESULTS

The data collected and processed produces a quantitative analysis of the effects lower-tropospheric wildfire conditions have on L1 band SNR. Utilizing RINEX data from non-wildfire and wildfire conditions at two base stations, the magnitude of signal disruption was determined using the RMS for a 24-hour period during the 2020 August Complex Fire. To determine the role locality has on the intensity of measured signal disruption, a trigonometric model was developed to assess the relationship between signal elevation, distance to fire perimeter, and altitude of peak interference. From this analysis, it was determined tropospheric wildfire conditions produce a statistically significant effect on L1 SNR across an elevation angle between 5 and 50 degrees.

Multipath error is the greatest source of signal interference in GPS SNR (Dammalage, 2018), and therefore, was an important consideration in the data preprocessing. This was controlled for by reducing the dimensions of the data to shared time of satellite signal intercept and elevation angle. By ensuring time of received signal, signal elevation angle, and signal azimuth are consistent across the test conditions, the multipath error was controlled for. The relationship between multipath error and signal elevation angle can be observed by the trends in Figure 4 a & b. The multipath of P190 was greatest between 5 and 20 degrees, and between 5 and 10 degrees for P336. These graphs demonstrate a successful control of multipath error as the SNR trend at low signal elevations is consistent among the test conditions for both base stations.

Normalizing the SNR data was accomplished using RMS and RMS residual calculations. The RMS residuals represent the signal disruption anomaly produced by the wildfire condition, calculated using Equation 2. A negative RMS residual indicates greater signal interference anomaly. Results demonstrated that the lowest RMS residuals occurred at lower elevation angles. GPS signals at low signal elevation angles travel through a greater density of atmosphere

particulate matter, and therefore, should produce the greatest difference in RMS residuals during TWC (Leick, 2015). The average elevation angle for RMS residuals below three standard deviations of the mean was calculated using Equation 3. As originally hypothesized, the results demonstrated the lowest RMS residuals occurred in signal elevations below 20 degrees, as displayed in Table 3.1. With multipath controlled for, the results indicate the L1 signal was experiencing greater signal disruption anomalies during the presence of atmospheric aerosols produced by the wildfire smoke plume. A non-significant result would have indicated either a normalized distribution of lower SNR signals across all elevation angles, or no significant difference at all.

The CORS base station P336 demonstrated the highest level of signal interference from the wildfire conditions. Table 1.2 provides the summary statistics for SNR across all measured elevation angles, with a mean SNR 1.27 dB/Hz during the wildfire conditions. At 12.9km distance from the fire perimeter, the magnitude of signal interference differed from the other measured base station, P190. Table 1.1 provides the summary statistics of SNR for P190, with a mean decrease of 0.62 dB/Hz across the 5-to-50-degree elevation angle. A lower magnitude of signal interference was expected from this station given its increased distance to the fire perimeter. To test the strength of the relation between distance to fire perimeter and SNR have on magnitude of signal anomaly, a simple proportion was calculated. The proportional distance between the two base stations and wildfire perimeter, 30.4km P190 and 12.9km P336, is equal to 2.36. The proportional difference of mean SNR between the two base stations was 1.9. This calculation indicates the presence of a relationship between the distance of the base station and magnitude of signal interference as increasing distance results in lower signal disruption.

Understanding the differing results produced by the two base stations is fundamental in determining the effect of wildfire interference on L1 signals. The spatial relationship between elevation angle and distance is put into context with Equation 3, the semi-empirical model that determines the elevation angle of greatest signal disruption. P190, at a greater distance to the wildfire perimeter, had a lower mean signal elevation for SNR measurements three standard deviations below the RMS residual mean. As anticipated, the base station with a greater distance to the wildfire perimeter experienced the highest signal interference at a lower elevation angle. Additionally, the mean angle of greatest signal interference was used to determine the altitude of signal as it passed through the fire perimeter. The altitude of greatest signal interference for both stations were within the known vertical wildfire plume height of 5km. Table 3.1 displays these results. The semi-proportional decay in SNR anomaly per kilometer, and lower signal elevation angle of the base station at a greater distance, indicate locality to fire perimeter is an important factor in magnitude of signal disruption. Additionally, the spatial relationship between SNR residual, elevation angle, and wildfire perimeter distance, further substantiate the claim that tropospheric wildfire conditions are responsible for greater signal interference.

4. CONCLUSION

GNSS as remote sensing has potential to be a valuable tool for remotely sensing tropospheric wildfire conditions (TWC). The prevalence of continuously operating reference stations allows for the development of spatial relationships to be derived among SNR measurements between multiple base stations in proximity to a wildfire perimeter. Particularly relevant to the diverse topography of California, multipath error is unique to a base station's geographic location. The archival of historic RINEX data at a given base station provides the necessary information for detecting abnormal interference given each station's known SNR multipath signature. The versatility of information in RINEX files provides the relevant parameters for studying spatial-sensitive signal interference signatures. With a near real-time sampling rate, GNSS atmospheric remote sensing has a significantly greater temporal resolution over traditional spaceborne atmospheric remote sensing methods (Bracaglia, 2019). This study indicated statistically significant L1 band signal interference at CORS GPS base stations in locale to the 2020 August Complex Fire. Additionally, data indicated a spatial relationship between magnitude of signal interference, elevation angle, and distance to fire perimeter.

Wildfires in the state of California cost the state 148.5 billion dollars, approximately 0.7% of the state's GDP in the year 2018 (Wang et. al, 2020). Increasing frequency and intensity of wildfires pose a threat to life and property. The public health implications of wildfire smoke propagation are significant, particularly to individuals sensitive to breathing atmospheric particulate. Individuals with heart, cardiovascular, and respiratory diseases, as well as children and pregnant women, are at elevated risk of serious health effects due to the inhalation of elevated atmospheric particulate matter concentrations (EPA, 2019). Public access to air quality information during wildfires is the primary method in which people in at-risk areas make

decisions regarding their respiratory health. Accuracy and relevance of air quality data, consequently, is important to public health. Incorporating GNSS-based measurements of wildfire smoke density and spatial distribution to preexisting methods of measuring air quality has the potential to increase public safety amid tropospheric wildfire conditions. Current methods of measuring smoke density and air quality suffer from a poor temporal resolution. The satellite platform VIIRS that observes atmospheric particle density has an overlapping scene time of 16 days (Bracaglia, 2019). Additionally, air quality monitoring stations update hourly (EPA, 2016). GNSS-based smoke density measurements can overcome these challenges with real time information, increasing the general public's ability to react to wildfire smoke dynamics.

The relationship established in this study between SNR of L1 band GPS signals and wildfire conditions substantiated the efficacy for utilizing GNSS as a method to remotely sense TWC. With a foundation for further research on the subject, there is much to be considered in future applications of L1 SNR TWC remote sensing. The intensity and burn area of a wildfire are fundamental factors in the density of atmospheric aerosols. This study focused on the conditions produced by the 2020 August Complex Fire due to its attribute of being the largest wildfire in California history. This simulated a worst-case scenario for tropospheric signal interference due to TWC. Due to the theoretical cutoff in which TWC can no longer be measured by L1 SNR anomalies, the efficacy of this method for remotely sensing moderate to small size wildfires remains unknown. The behavior of smoke propagation through the atmosphere is variable among wildfire intensity, location, and meteorological conditions. While these variables are consistent and known in a case-study, they represent a challenge for real time TWC GNSS-based remote sensing.

An additional variable of concern is ionospheric interference. Global ionospheric maps (GIM) measure vertical ionospheric delay of GPS signals for a given location of signal reception. Significant changes in total electron content (TEC) have limited variability over a fixed non-polar location, however, seasonal variability of solar radiation, solar flares, and short-term changes to regional TEC morphology pose a risk to disrupting TWC signal interference models (Leick, 2015). Particularly, ionospheric interference would be most destructive in small to moderate scale GNSS TWC remote sensing applications. Further research on TWC signal interference should incorporate GIM data to subtract ionospheric interference from tropospheric interference to ensure the least amount of potential variability in SNR.

BIBLIOGRAPHY

Bracaglia, M., Volpe, G., Colella, S., Santoleri, R., Braga, F., & Brando, V. E. (2019). Using overlapping VIIRS scenes to observe short term variations in particulate matter in the coastal environment. *Remote Sensing of Environment*, *233*, 111367. https://doi.org/10.1016/j.rse.2019.111367

Cal Fire. (2021, October 6). Top 20 Largest California Wildfires. https://www.fire.ca.gov/media/4jandlhh/top20_acres.pdf

Dammalage, T. L. (2018). The effect of multipath on single frequency c/a code based gps positioning. *Engineering, Technology & Applied Science Research*, *8*(4), 3270–3275. https://doi.org/10.48084/etasr.2206

gwalyne_NASA. (2020) . Plume Height (MISR) on 8/24/20 for the California Fires 202o https://services7.arcgis.com/WSiUmUhlFx4CtMBB/arcgis/rest/services/California_Fires_Plume_Data_MISR_ASL/FeatureServer

Larson, K. (2018, January 11). Analyzing the gnss data. https://www.kristinelarson.net/analyzing-the-data/

Larson, K. (2021). Gnssrefl GitLab. https://www.unavco.org/gitlab/gnss_reflectometry/gnssrefl/-/blob/master/README.md#module1

Larson, K. M., Palo, S., Roesler, C., Mattia, M., Bruno, V., Coltelli, M., & Fee, D. (2017). Detection of plumes at Redoubt and Etna volcanoes using the GPS SNR

method. *Journal of Volcanology and Geothermal Research, 344*, 26-39. doi:10.1016/j.jvolgeores.2017.04.005

Lau, L., & He, J. (2017). Investigation into the effect of atmospheric particulate matter (PM2.5 and PM10) concentrations on gps signals. Sensors (Basel, Switzerland), 17(3), 508. https://doi.org/10.3390/s17030508

Leick, A., Rapoport, L., & Tatarnikov, D. (2015). *Gps satellite surveying: Leick/gps satellite surveying*. John Wiley & Sons, Inc. https://doi.org/10.1002/9781119018612

Li, Y., Tong, D. Q., Ngan, F., Cohen, M. D., Stein, A. F., Kondragunta, S., et al. (2020). Ensemble $PM_{2.5}$ forecasting during the 2018 Camp Fire event using the HYSPLIT transport and dispersion model. *Journal of Geophysical Research: Atmospheres*, 125, e2020JD032768. https://doi.org/10.1029/2020JD032768

Mphale, K. (2005). RADIOWAVE PROPAGATION MEASUREMENTS AND PREDICTION IN BUSHFIRES. James Cook University. https://researchonline.jcu.edu.au/2028/2/02whole.pdf

T.Takasu. Jan 19, 2018. RTKLIB: An Open Source Program Package for GNSS Positioning. http://www.rtklib.com/

US EPA, O. (2016, August 30). *Air data basic information* [Data and Tools]. https://www.epa.gov/outdoor-air-quality-data/air-data-basic-information

US EPA, O. (2019, August 13). *Which Populations Experience Greater Risks of Adverse Health Effects Resulting from Wildfire Smoke Exposure?* [Overviews and Factsheets].

https://www.epa.gov/wildfire-smoke-course/which-populations-experience-greater-risks-adverse-health-effects-resulting

Wang, D., Guan, D., Zhu, S., Kinnon, M. M., Geng, G., Zhang, Q., Zheng, H., Lei, T., Shao, S., Gong, P., & Davis, S. J. (2021). Economic footprint of California wildfires in 2018. *Nature Sustainability, 4*(3), 252–260. https://doi.org/10.1038/s41893-020-00646-7

Yang, Lei, et al. (2021) "Analysis of Precipitable Water Vapour Characteristics from GNSS Measurements during the Snow Season in Liaoning Province, China." *Advances in Space Research*, vol. 67, no. 8, 2021, pp. 2347–2358., doi:10.1016/j.asr.2021.01.026.